Biosensors and Bioelectronics 81 (2016) 303–308

Contents lists available at ScienceDirect

Biosensors and Bioelectronics

journal homepage: www.elsevier.com/locate/bios

Label-free and enzyme-free colorimetric detection of microRNA by catalyzed hairpin assembly coupled with hybridization chain reaction

Hao Wu*, Yaling Liu, Hongyong Wang, Jun Wu, Feifan Zhu, Pei Zou*

Key Laboratory of Nuclear Medicine, Ministry of Health, Jiangsu Key Laboratory of Molecular Nuclear Medicine, Jiangsu Institute of Nuclear Medicine, Wuxi, Jiangsu 214063, China

ARTICLE INFO

Article history:
Received 6 January 2016
Received in revised form
1 March 2016
Accepted 8 March 2016
Available online 9 March 2016

Keywords:
miRNA
Dual signal amplification
Colorimetric biosensor
Split G-quadruplex structure
DNAzyme

ABSTRACT

In this study, a simple, label-free, and enzyme-free colorimetric biosensor has been developed for amplified detection of let-7a microRNA (miRNA) on the basis of dual signal amplification strategy. The sensing system mainly consists of four unlabeled hairpin probes termed H1, H2, H3, and H4. Upon sensing of the target miRNA, hairpin H1 is opened. Then hairpin H2 hybridizes with H1 forming H1–H2 duplex and frees the target miRNA that can be recycled to trigger another reaction cycle. In addition, the newly formed H1–H2 duplex hybridizes with hairpin H3, and this triggers the autonomous cross-opening of the two hairpins H3 and H4 through hybridization chain reaction. During this process, numerous split G-quadruplex structures are generated and further associate with cofactor hemin to form massive peroxidase-mimicking DNAzymes. The resulting DNAzymes catalyze the H_2O_2-mediated oxidation of colorless 2,2′-azino-bis(3-ethylbenzothiazoline-6-sulfonic acid) ($ABTS^{2-}$) to the green-colored $ABTS^{\bullet-}$, inducing a remarkably amplified colorimetric signal. This newly developed sensing system exhibits high sensitivity toward miRNA with a detection limit of 7.4 fM and a large dynamic range of 6 orders of magnitude from 10 fM to 10 nM. Furthermore, it exhibits a good performance to discriminate single-base difference among the miRNA family members and holds a great potential for early diagnosis in gene-related diseases.

1. Introduction

MicroRNAs (miRNAs) are a class of 19–23 nucleotides single-stranded noncoding RNA molecules that regulate gene expressions at the post-transcriptional level (Huang et al., 2013a, 2013b). It has been demonstrated that miRNAs play critical regulatory functions in many physiological processes, such as cell differentiation, proliferation, and apoptosis (Huang et al., 2013a, 2013b; Ye et al., 2015). There is increasing evidence showed that aberrant expression of certain miRNAs is closely associated with various diseases, especially cancers (Huang et al., 2013a, 2013b; Hou et al., 2015). For instance, miRNA-21 has been found to be overexpressed in many cancer tissues, including gastric, breast, lung, colorectal, and prostate cancers (Lu et al., 2008; Medina and Slack, 2008; Huang et al., 2013a, 2013b). Therefore, miRNA expression and quantitative profiles can be employed as biomarkers for early diagnosis of cancers (Wang et al., 2015; Shi et al., 2015). Several traditional methods have been utilized for miRNA detection, including Northern blotting (Houbaviy et al., 2003; Valoczi et al., 2004), quantitative reverse transcription polymerase chain reaction (qRT-PCR) (Raymond et al., 2005; Shi and Chiang, 2005), and microarrays (Liu et al., 2004; Thomson et al., 2004). However, these miRNA detection techniques are complicated, expensive, and time-consuming, which have intrigued recent development of simple and new signal amplification strategies for miRNA detection (Shi et al., 2015). Alternatively, catalyzed hairpin assembly has recently been developed for DNA nanostructure organization (Yin et al., 2008; Li et al., 2012). Also, it can be served as a promising enzyme-free signal amplification strategy for DNA detection (Allen et al., 2012; Liu et al., 2013; Jiang et al., 2014; Wu et al., 2015a, 2015b). Therefore, the exploration of catalyzed hairpin assembly amplification without the involvement of any enzymes will potentially simplify the detection of miRNA.

Very recently, great attention has been focused on isothermal signal amplification without using of protein enzymes, such as by employing catalytic nucleic acids as amplified indicators (Ren et al., 2014; Liu et al., 2015). DNAzyme are a class of catalytic nucleic acids which are isolated from an in vitro selection process termed systematic evolution of ligands by exponential enrichment (SELEX) (Willner et al., 2008; Huang et al., 2013a, 2013b). The flexibility to encode in the base sequences of DNA functional and structural information makes DNAzymes ideal biocatalysts for

* Corresponding author.
E-mail addresses: wuhao@jsinm.org (H. Wu), zoupei@jsinm.org (P. Zou).

http://dx.doi.org/10.1016/j.bios.2016.03.013
0956-5663/

bioanalytical applications (Shimron et al., 2012). G-quadruplex/hemin DNAzyme as one of DNAzymes has received increasing interest and concern in recent years (Zhang et al., 2011). The G-quadruplex/hemin DNAzyme exhibits peroxidase-like activity and can effectively catalyze the H_2O_2-mediated oxidation of 2,2′-azino-bis(3-ethylbenzothiazoline-6-sulfonic acid) ($ABTS^{2-}$) (Travascio et al., 1998) or 5-amino-2,3-dihydro-1,4-phthalazinedione (luminol) (Pavlov et al., 2004), accompanied by a color change or chemiluminescence emission. With these properties, the G-quadruplex/hemin DNAzyme has been extensively used as a catalytic label for amplified colorimetric (Wang et al., 2014; Verga et al., 2015) or chemiluminescence (Gao and Li, 2013, 2014) detection of biomolecules.

As far as we know, there are few reports about the detection methods which combine the two amplification strategies of catalyzed hairpin assembly and hybridization chain reaction. Enlightened by the above fact, we challenged the combination of these two amplification strategies to develop a new biosensing system. Hence, in this work we develop for the first time a simple, label-free, and enzyme-free G-quadruplex DNAzyme-based colorimetric biosensing system that ingeniously combines catalyzed hairpin assembly and hybridization chain reaction for sensitive detection of miRNAs. The integration of these two amplification strategies not only improves the sensitivity of the biosensing system but also provides a new way for catalyzed hairpin assembly amplification technology to detect miRNAs. As proof of concept, detection of let-7a miRNA is demonstrated in this study. The assay does not involve any protein enzyme and need any chemical modification, which is simple and cost-effective. With the significant dual signal amplifications, the newly developed sensing system can detect target miRNA with an extremely low detection limit of 7.4 fM and it can discriminate single-base difference among the miRNA family members. Given the high-performance for miRNA analysis, this sensing system has great potential to be applied in biochemical research and clinical diagnosis.

2. Experimental section

2.1. Reagents and chemicals

HPLC-purified miRNAs and PAGE-purified DNA oligonucleotides were obtained from Genscript (Nanjing) Co., Ltd. (Jiangsu, China). Ribonuclease (RNase) inhibitor and diethylprocarbonate (DEPC)-treated deionized water were purchased from Shanghai Sangon Biotechnology Co., Ltd. (Shanghai, China). Human lung total RNA (100 μg/100 μL) was purchased from Thermo Fisher Scientific (China) Co., Ltd. [Tris(hydroxymethy-l)aminomethane] (Tris), 4-(2-hydroxyethyl)piperazine-L-ethanesulfonic acid sodium salt (HEPES), hemin, 2,2-azino-bis(3-ethylbenzothiozoline-6-sulfonic acid) diammonium salt (ABTS), and H_2O_2 were purchased from Aladdin Reagents (Shanghai) Co., Ltd. (Shanghai, China). Other chemicals were obtained from Sinopharm Chemical Reagent Co., Ltd. (Shanghai, China). MiRNAs were diluted to appropriate concentrations with DEPC-treated water, and DNA oligonucleotides were diluted with 20 mM Tris–HCl buffer (200 mM NaCl, 2 mM MgCl2, and 20 mM KCl, pH=7.4) to give stock solutions of 100 μM. Each DNA oligonucleotide was heated to 95 °C for 5 min, and then slowly cooled down to room temperature before use. A stock solution of hemin (1 mM) was prepared by dissolving 6.5 mg of hemin in 10 mL of dimethyl sulfoxide (DMSO) and stored at −20 °C in the dark. DEPC-treated deionized water was used throughout the work. The sequences of the oligonucleotides are listed in Table S1.

2.2. Procedure for miRNA assay

The experiments were carried out in 50 μL of solution containing 10 μL of H1 (0.5 μM), 10 μL of H2 (0.5 μM), 10 μL of H3 (2.5 μM), 10 μL of H4 (2.5 μM), 5 μL of RNase inhibitor (10 U), and 5 μL of target miRNA (varying concentrations), followed by incubating at 37 °C for 90 min. After incubation, the solution was diluted with 120 μL HEPES buffer (25 mM HEPES, 200 mM NaCl, 20 mM KCl, and 1% DMSO, pH=7.4). Subsequently, 10 μL of hemin (10 μM) was added into the above solution and incubated at room temperature for 60 min. Finally, 10 μL of ABTS (40 mM) and 10 μL of H_2O_2 (40 mM) were added to the mixture to yield a total volume of 200 μL. After incubation for 5 min, the resulting samples were used for absorbance measurements.

2.3. Absorbance measurements

Absorbance measurements were recorded with a SpectraMax M5e Multi-Mode Microplate Reader (Molecular Devices, CA, USA). The absorption spectra of the solution were collected from 390 to 480 nm with a step of 2 nm.

3. Results and discussion

3.1. Design of hairpin probes for dual signal amplification

The sensing system mainly consists of four unlabeled hairpin probes termed H1, H2, H3, and H4. Hairpin H1 contains two domains identified as I and II according to their different functions. Domain I (pink) is the recognition sequence for the target miRNA and is partially caged in the duplex structure of the stem by hybridization with domain II (skyblue). Hairpin H2 includes three domains. Domains II′ (skyblue) and I′ (pink) are complementary to domains II and I in H1, respectively. Domain III′ (blue) consists of a sequence that is complementary to domain III in H3 that, upon hybridization, triggers the autonomous cross-opening of the two hairpins H3 and H4. Hairpin H3 is functionalized at its 5′ end with three-fourths of the G-quadruplex sequence, domain V (green), linked to the programmed sequence composed of domains IV (red) and III (blue). The 3′ end of H3 consists of a sequence comprising of one-fourth of the G-quadruplex sequence, domain VI (green). In hairpin H3, domain III is partially hybridized with domains IV and V at the stem region, resulting in a stable hairpin configuration in an initially locked format. Hairpin H4 includes four domains: one-fourth of the G-quadruplex sequence (domain VI) at the 5′ end, programmed sequences of domains IV′ and III′ that are complementary to domains IV and III in H3, respectively, and three-fourths of the G-quadruplex sequences (domain V) at the 3′ end. It should be noted that domain V (three-fourths of the G-quadruplex sequence) is partially caged in the duplex of the stem in both hairpin H3 and H4. As a result, two split G-quadruplex segments (one-fourth and three-fourths of the G-quadruplex sequences in H3 or H4) are prohibited to self-assemble into the split G-quadruplex structure (Shimron et al., 2012; Wu et al., 2015a, 2015b).

3.2. Principle of dual signal amplification strategy for miRNA detection

The new colorimetric sensing system for amplified detection of miRNA is illustrated in Scheme 1. In the absence of the target miRNA, the four hairpin probes (H1, H2, H3, and H4) can coexist in solution and keep their stable hairpin conformation, which provides a low background for the sensing system. Upon the interaction of domain I with the target miRNA (T), hairpin H1 is opened, result in the exposure of domain II. The exposed domain II

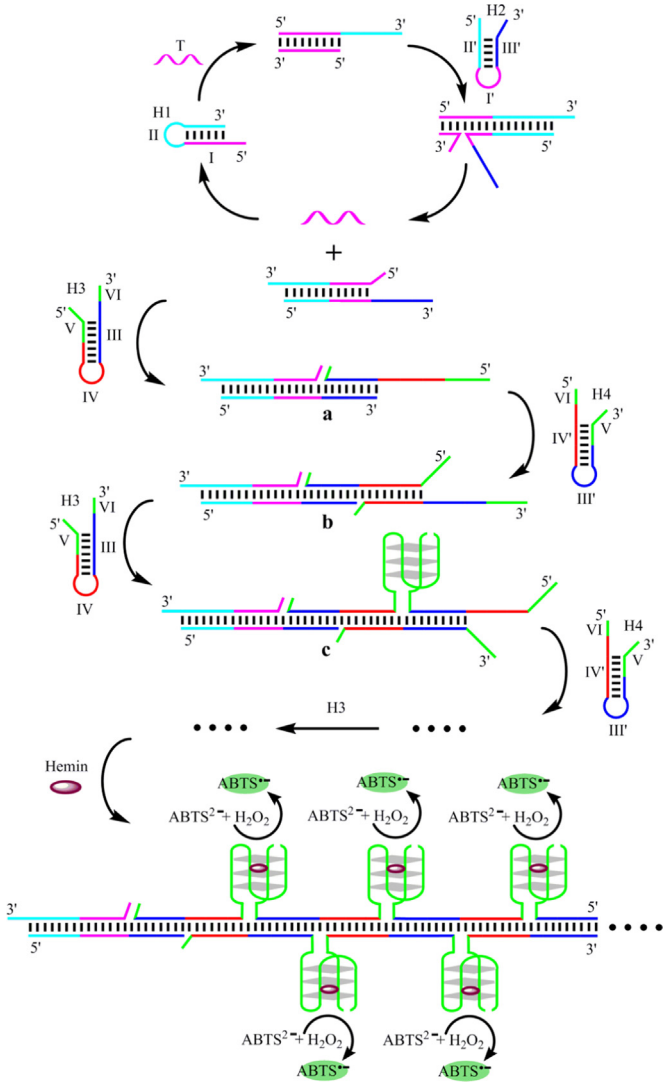

Scheme 1. Principle of dual signal amplification strategy for highly sensitive detection of miRNA.

serves as a toehold to hybridize with hairpin H2. Since H1–H2 duplex is more stable than H1–T duplex, the target miRNA can be displaced from H1 by H2 through a process similar to DNA branch migration (Li et al., 2011). The displaced target miRNA again binds with a new hairpin H1 to initiate the target recycling amplification cycle. As a result, each copy of target miRNA can trigger numerous assembly processes between hairpins H1 and H2. Moreover, the newly formed H1–H2 duplex can be further used as a primer to initiate hybridization chain reaction between hairpins H3 and H4. Specifically, the liberated domain III′ in H1–H2 duplex can hybridize with the stem region of H3, domain III, leading to an opening of H3 and the generation of structure a. The opening of H3 releases the domain IV and the conserved three-fourths of the G-quadruplex sequence (domain V). The released domain IV in structure a then hybridizes with domain IV′ in hairpin H4, and opens H4 to yield structure b. Subsequently, the resulting structure b cross-hybridizes with hairpin H3 via hybridization chain reaction. This results in structure c, where two split G-quadruplex segments (domains V and VI) self-assemble into the split G-quadruplex structure (Shimron et al., 2012; Wu et al., 2015a, 2015b). In the process of autonomous cross-opening of hairpins H4 and H3, hybridization chain reaction can be repeated continuously, generating a large number of split G-quadruplex structures. These split G-quadruplex structures interact with cofactor hemin to form massive peroxidase-mimicking DNAzymes that catalyze the H_2O_2-mediated oxidation of colorless $ABTS^{2-}$ to green-colored $ABTS^{\bullet-}$, thus providing the amplified colorimetric detection of the target.

3.3. Amplification effect of dual signal amplification strategy

To prove the signal amplification effect by dual signal amplification strategy (catalyzed hairpin assembly coupled with hybridization chain reaction), another two split G-quadruplex segments G1 and G2 (where G1 and G2 are single-stranded DNA sequence containing three-fourths and one-fourth of G-quadruplex, respectively) were also designed for comparison. Upon the recognition of the target miRNA, hairpin H1 is opened, making it available for hybridization with hairpin H2. Then, the target miRNA can be displaced from H1 by H2 through a branch migration process (Li et al., 2011). The released target miRNA can participate in the next hairpin assembly process. Meanwhile, the newly formed H1–H2 duplex draws the two split G-quadruplex segments G1 and G2 together to self-assemble into the split G-quadruplex structure that can bind with cofactor hemin to yield a colorimetric signal (Fig. 1A). It could be denoted as a typical catalyzed hairpin assembly strategy. To highlight the amplification effect, the target miRNA at a concentration of 10 nM was analyzed by the two sensing system outlined in Scheme 1 and Fig. 1A, respectively. As shown in Fig. 1B, in the absence of the target miRNA, two sensing

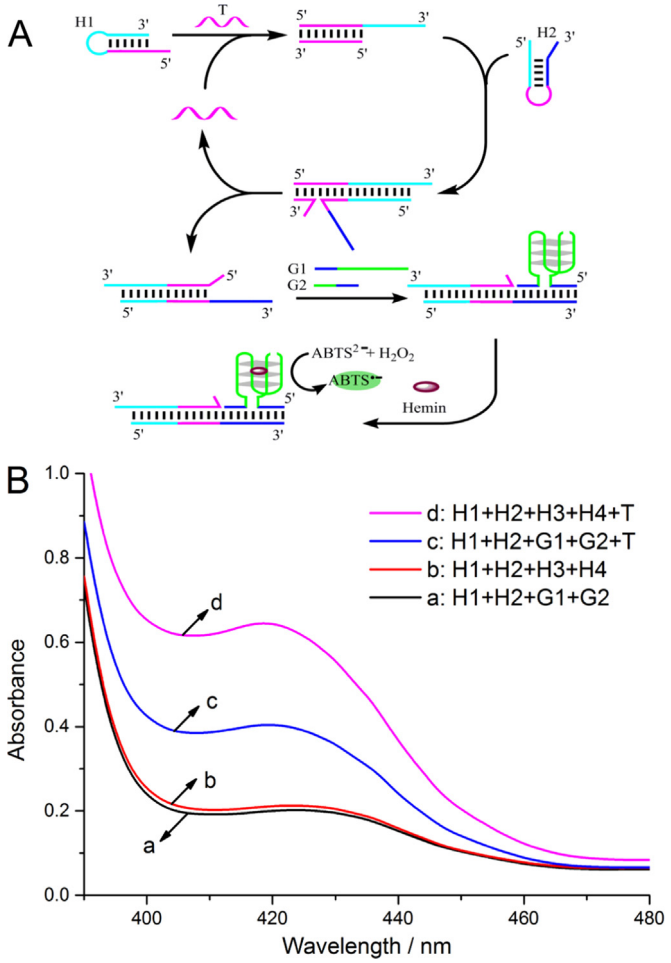

Fig. 1. (A) Schematic illustration of typical catalyzed hairpin assembly strategy for detection of miRNA. (B) Absorption spectra of sample solutions under different conditions: (a) H1 (25 nM), H2 (25 nM), G1 (125 nM), G2 (125 nM); (b) H1 (25 nM), H2 (25 nM), H3 (125 nM), H4 (125 nM); (c) H1 (25 nM), H2 (25 nM), G1 (125 nM), G2 (125 nM), T (10 nM); (d) H1 (25 nM), H2 (25 nM), H3 (125 nM), H4 (125 nM), T (10 nM). Experimental conditions: hemin 500 nM, ABTS 2 mM, and H_2O_2 2 mM.

system showed almost the same colorimetric response (curve a, b). When the target miRNA was introduced into the system, an obvious signal enhancement could be observed due to the typical catalyzed hairpin assembly strategy (curve c). In contrast, the colorimetric response to the target miRNA by the dual signal amplification strategy at the same concentration was significantly higher than that by the typical catalyzed hairpin assembly strategy (curve d). The results strongly indicate this dual signal amplification strategy is efficient for amplified detection of target miRNA.

3.4. Optimization of experimental conditions

The performance of the developed colorimetric sensing system is strongly influenced by the assay conditions such as the concentration of the four hairpin probes and the amplification reaction time. To optimize the concentration of the two hairpins H1 and H2, 10 nM target miRNA was examined with different probe concentrations by the sensing system outlined in Fig. 1A. As shown in Fig. S1, the best signal to background ratio was obtained when 25 nM of each hairpin probes (H1 and H2) was used. Thus we fixed the hairpin H1 and H2 concentration at 25 nM each and used for the following experiments. We further optimized the concentration of the hairpins H3 and H4. The experiments were performed by exposing 10 nM target miRNA, 25 nM H1, and 25 nM H2 to varying concentrations of H3 and H4 to reach a ratio from 1:2 to 1:6. The experimental results in Fig. S2 showed that probe ratio of 1:5 performed better than the other four groups. Thus, the concentration of hairpin H3 and H4 was fixed at 125 nM each and used for the following experiments. In this assay, the amplification reaction time is another important factor can significantly affect the performance of the sensing system. As such, the influence of amplification reaction time upon the colorimetric signal was further investigated. As shown in Fig. S3, the colorimetric signal increased with a longer time of incubation before reaching saturation after 90 min. This is consistent with the fact that a longer reaction time will undoubtedly result in larger numbers of split G-quadruplex structures for enhanced signal amplification. By weighing both the sensitivity and the total assay time, the amplification reaction time of 90 min was selected for the following experiments.

3.5. Analytical performance of dual signal amplification strategy for miRNA detection

To demonstrate the sensitivity of the developed sensing system, target miRNA with different concentrations was measured under the optimal experimental conditions. Fig. 2A shows the variance of absorption intensity with the concentration of target miRNA. As the concentration of target miRNA increases, large numbers of split G-quadruplex/hemin DNAzymes are generated, resulting in the increase of absorption intensity correspondingly. An exponential curve is obtained between the absorption intensity and the concentration of target miRNA from 10 fM to 10 nM (Fig. 2B). Notably, in logarithmic scales, the absorption intensity exhibits a good linear correlation with the concentration of target miRNA over a range of 6 orders of magnitude from 10 fM to 10 nM (inset of Fig. 2B). The regression equation is $A=0.56787+0.07301\log_{10}C$ with a correlation coefficient of 0.9896, where A and C represent the absorption intensity and the concentration of target miRNA, respectively. Based on the 3σ calculation, the detection limit is estimated to be 7.4 fM. The sensitivity of the sensing system was compared to other miRNA detection methods based on catalyzed hairpin assembly amplification strategy in Table S2. In addition, Table S3 compares the performance of the sensing system to some previous miRNA detection methods based on different signal amplification strategies.

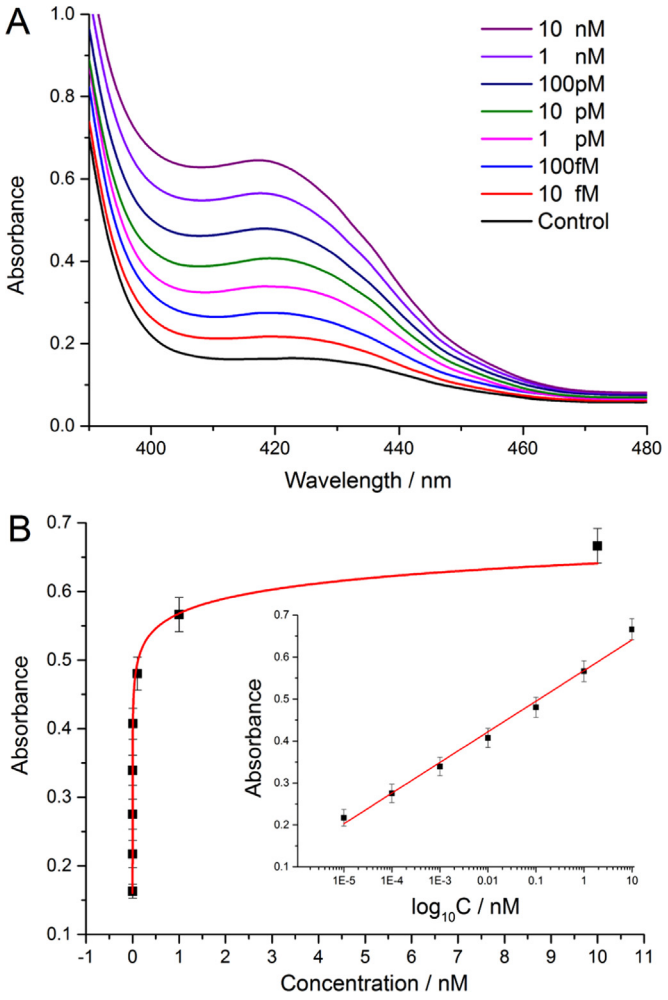

Fig. 2. (A) Absorption spectra corresponding to the analysis of target let-7a miRNA at different concentrations. (B) Dependence of absorption intensity on the target miRNA concentration. Inset shows the linear relationship between the absorption intensity and the log of concentrations of target miRNA from 10 fM to 10 nM. Experimental conditions: H1 25 nM, H2 25 nM, H3 125 nM, H4 125 nM, hemin 500 nM, ABTS 2 mM, and H_2O_2 2 mM. The error bars represent the standard deviations of three parallel tests.

It revealed that the dual signal amplification strategy proposed in this work possessed the feature of low detection limit. Such high sensitivity of the sensing system can be attributed to the high amplification efficiency of the dual signal amplification strategy based on the ingenious combination of catalyzed hairpin assembly and hybridization chain reaction.

3.6. Specificity of dual signal amplification strategy for miRNA detection

A great challenge for an excellent miRNA assay is its ability to distinguish the miRNA family members with high sequence homology. The let-7 miRNA family members consist of eight highly similar miRNAs that differ by only 1–4 nucleotide from each other (Zhang et al., 2014). To further evaluate the specificity of the sensing system, we performed a series of contrast experiments using four kinds of let-7 miRNA family members, including perfectly matched let-7a, two-bases mismatched let-7b, single-base mismatched let-7c, four-bases mismatched let-7i, and a sample without target as a blank control. The results are displayed in Fig. 3. One can see that target let-7a miRNA can be clearly distinguished against other let-7 miRNA family members. Judging from the histogram (Fig. 3B), the absorption intensity of two-bases

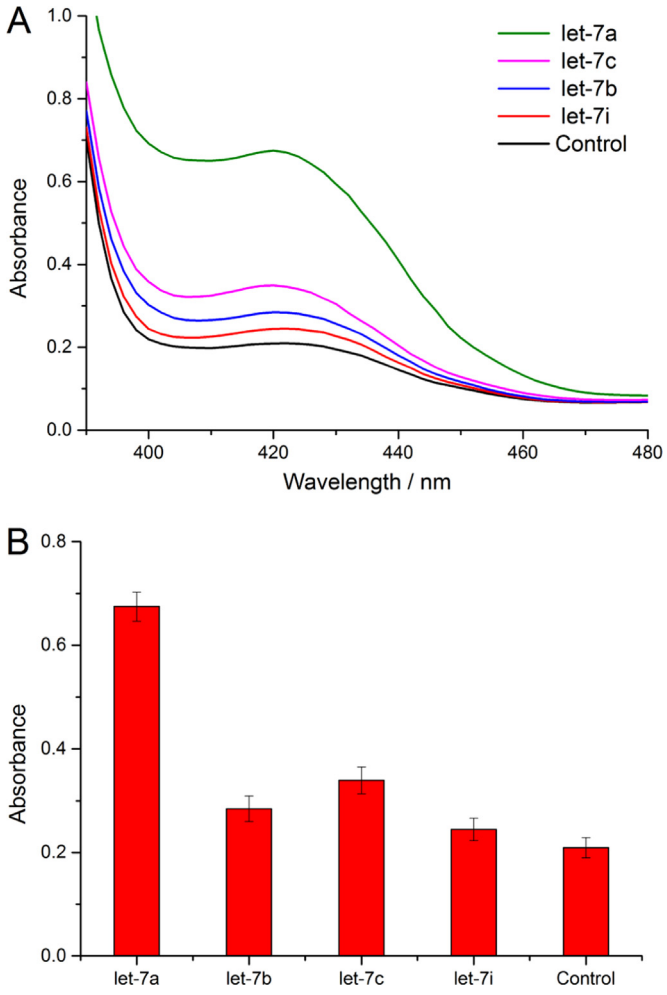

Fig. 3. Specificity of miRNA assay. (A) Absorption spectra in response to let-7a (green), let-7b (blue), let-7c (pink), let-7i (red), and the control samples (black). (B) Variance of absorption intensity in response to let-7a, let-7b, let-7c, let-7i, and the control samples. Experimental conditions: H1 25 nM, H2 25 nM, H3 125 nM, H4 125 nM, hemin 500 nM, ABTS 2 mM, and H_2O_2 2 mM. The error bars represent the standard deviations of three parallel tests. (For interpretation of the references to color in this figure legend, the reader is referred to the web version of this article.)

mismatched let-7b, single-base mismatched let-7c, and four-bases mismatched let-7i was only about 42.13%, 50.31% and 36.25% of that of perfectly matched let-7a miRNA, respectively. These results demonstrate the capability of the sensing system to discriminate perfectly matched miRNA target from mismatched miRNAs, suggesting the high specificity of the sensing system for miRNA assay.

3.7. *Determination of miRNA in total RNA sample*

To verify the effectiveness of the assay in real biological samples analysis, we measured the level of let-7a in total RNA sample. Human lung total RNA (100 μg/100 μL) was diluted to 50 ng/μL with Tris–HCl buffer. Afterwards, aliquots of the diluted RNA sample (1 μL) were spiked with standard solutions containing let-7a at concentrations of 0, 5, 10, 15, 20, 25 pM in reaction volume of 50 μL respectively. Next, the dual amplification reaction and colorimetric detection were performed as described in the experimental section. As shown in Fig. S4, the absorption intensities increased with increasing the spiked concentrations of let-7a over the range of 0.1–0.5 pM. The content of let-7a estimated by standard addition method was 0.292 pM in a real sample containing 5 ng total RNA in the volume of 200 μL. It was calculated that the concentration of let-7a in original sample was 11.68 nM. The results demonstrate that the sensing system holds a great promise for real sample analysis.

4. Conclusions

In conclusion, we have developed a simple and highly sensitive colorimetric biosensor for amplified detection of miRNA by catalyzed hairpin assembly coupled with hybridization chain reaction. This assay has several excellent features. First, the assay does not need any protein enzyme and chemical modification, which makes it enzyme-free, label-free, and cost-effective. Second, the whole reaction is conducted in an isothermal homogeneous solution without requiring troublesome separation procedures and time-consuming thermal cycling. Third, the newly developed sensing system exhibits high sensitivity toward target miRNA with a detection limit of 7.4 fM and a large dynamic range of 6 orders of magnitude. Finally, this sensing system has a good performance to discriminate single-base difference among the miRNA family members and holds a great potential for early diagnosis in gene-related diseases.

Acknowledgment

This work is supported by the Social Development Fund of Jiangsu Province (BE2013615).

Appendix A. Supporting information

Supplementary data associated with this article can be found in the online version at http://dx.doi.org/10.1016/j.bios.2016.03.013.

References

Allen, P.B., Arshad, S.A., Li, B., Chen, X., Ellington, A.D., 2012. Lab. Chip 12, 2951–2958.
Gao, Y., Li, B., 2013. Anal. Chem. 85, 11494–11500.
Gao, Y., Li, B., 2014. Anal. Chem. 86, 8881–8887.
Hou, T., Li, W., Liu, X., Li, F., 2015. Anal. Chem. 87, 11368–11374.
Houbaviy, H.B., Murray, M.F., Sharp, P.A., 2003. Dev. Cell 5, 351–358.
Huang, Y., Chen, J., Zhao, S., Shi, M., Chen, Z.F., Liang, H., 2013a. Anal. Chem. 85, 4423–4430.
Huang, Y., Yang, Y.B., Zhang, X.H., Yu, X.L., Wang, Z.B., Cheng, X.C., 2013b. Med. Oncol. 30, 376.
Jiang, Y.S., Bhadra, S., Li, B., Ellington, A.D., 2014. Angew. Chem. Int. Ed. 126, 1876–1879.
Li, B.L., Ellington, A.D., Chen, X., 2011. Nucleic Acids Res. 39, e110.
Li, B.L., Jiang, Y., Chen, X., Ellington, A.D., 2012. J. Am. Chem. Soc. 134, 13918–13921.
Liu, C.G., Calin, G.A., Meloon, B., Gamliel, N., Sevignani, C., Ferracin, M., Dumitru, C. D., Shimizu, M., Zupo, S., Dono, M., Alder, H., Bullrich, F., Negrini, M., Croce, C.M., 2004. Proc. Natl. Acad. Sci. USA 101, 9740–9744.
Liu, S., Cheng, C., Gong, H., Wang, L., 2015. Chem. Commun. 51, 7364–7367.
Liu, S., Wang, Y., Ming, J., Lin, Y., Cheng, C., Li, F., 2013. Biosens. Bioelectron. 49, 472–477.
Lu, Z., Liu, M., Stribinskis, V., Klinge, C.M., Ramos, K.S., Colburn, N.H., Li, Y., 2008. Oncogene 27, 4373–4379.
Medina, P.P., Slack, F.J., 2008. Cell Cycle 7, 2485–2492.
Pavlov, V., Xiao, Y., Gill, R., Dishon, A., Kotler, M., Willner, I., 2004. Anal. Chem. 76, 2152–2156.
Raymond, C.K., Roberts, B.S., Garrett-Engele, P., Lim, L.P., Johnson, J.M., 2005. RNA 11, 1737–1744.
Ren, R., Wang, L.L., Ding, T.R., Li, X.M., 2014. Biosens. Bioelectron. 54, 122–127.
Shi, K., Dou, B., Yang, C., Chai, Y., Yuan, R., Xiang, Y., 2015. Anal. Chem. 87, 8578–8583.
Shi, R., Chiang, V.L., 2005. Biotechniques 39, 519–525.
Shimron, S., Wang, F., Orbach, R., Willner, I., 2012. Anal. Chem. 84, 1042–1048.
Thomson, J.M., Parker, J., Perou, C.M., Hammond, S.M., 2004. Nat. Methods 1, 47–53.
Travascio, P., Li, Y., Sen, D., 1998. Chem. Biol. 5, 505–517.
Valoczi, A., Hornyik, C., Varga, N., Burgyan, J., Kauppinen, S., Havelda, Z., 2004. Nucleic Acids Res. 32, e175.
Verga, D., Welter, M., Steck, A.L., Marx, A., 2015. Chem. Commun. 51, 7379–7381.

Wang, F., Lu, C.H., Liu, X., Freage, L., Willner, I., 2014. Anal. Chem. 86, 1614–1621.
Wang, T., Viennois, E., Merlin, D., Wang, G., 2015. Anal. Chem. 87, 8173–8180.
Willner, I., Shlyahovsky, B., Zayats, M., Willner, B., 2008. Chem. Soc. Rev. 37, 1153–1165.
Wu, H., Liu, Y., Wang, H., Wu, J., Zhu, F., Zou, P., 2015a. Biosens. Bioelectron. 66, 277–282.
Wu, H., Zhang, K., Liu, Y., Wang, H., Wu, J., Zhu, F., Zou, P., 2015b. Biosens. Bioelectron. 64, 572–578.
Ye, S., Wu, Y., Zhai, X., Tang, B., 2015. Anal. Chem. 87, 8242–8249.
Yin, P., Choi, H.M.T., Calvert, C.R., Pierce, N.A., 2008. Nature 451, 318–323.
Zhang, L., Zhu, J., Li, T., Wang, E., 2011. Anal. Chem. 83, 8871–8876.
Zhang, P., Zhang, J., Wang, C., Liu, C., Wang, H., Li, Z., 2014. Anal. Chem. 86, 1076–1082.